ACS Medicinal Chemistry Letters

Letter

Cite This: ACS Med. Chem. Lett. 2018, 9, 114−119

^{18}F-Radiolabeled Panobinostat Allows for Positron Emission Tomography Guided Delivery of a Histone Deacetylase Inhibitor

Harikrishna Kommidi,[†] Umberto Tosi,[‡] Uday B. Maachani,[‡] Hua Guo,[†] Christopher S. Marnell,[‡] Benedict Law,[†] Mark M. Souweidane,[‡] and Richard Ting*[,†]

[†]Department of Radiology, Molecular Imaging Innovations Institute, Weill Cornell Medicine, New York, New York 10065, United States

[‡]Department of Neurological Surgery, Weill Cornell Medicine, New York, New York 10065, United States

Supporting Information

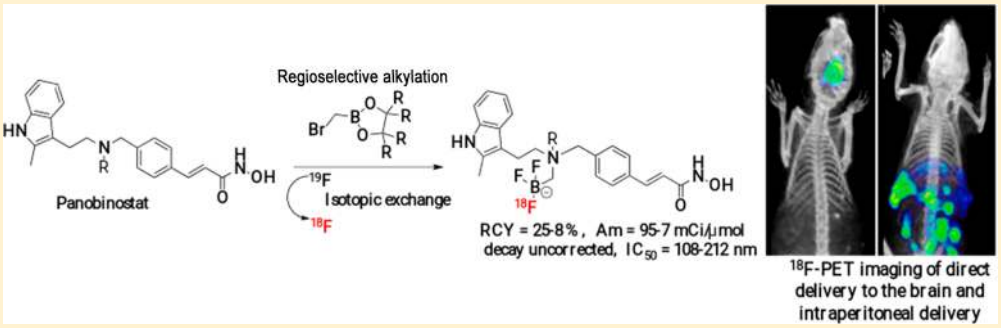

ABSTRACT: Histone deacetylase (HDAC) inhibition is becoming an increasingly popular approach to treat cancer, as HDAC overexpression is common in many malignancies. The blood−brain barrier (BBB) prevents systemically delivered drugs from reaching brain at effective concentration, making small-molecule-HDAC inhibition in brain tumors particularly challenging. To circumvent the BBB, novel routes for administering therapeutics are being considered in the clinic, and a need exists for drugs whose deliveries can be directly imaged, so that effective delivery across the BBB can be monitored. We report chemistry for radiolabeling the HDAC inhibitor, panobinostat, with fluoride-18 (compound-**1**). Like panobinostat, compound **1** retains nanomolar efficacy in diffuse intrinsic pontine glioma (DIPG IV and XIII) cells (IC_{50} = 122 and 108 nM, respectively), with lesser activity against U87 glioma. With a favorable therapeutic ratio, **1** is highly selective to glioma and demonstrates considerably less toxicity toward healthy astrocyte controls (IC_{50} = 5265 nM). Compound **1** is stable in aqueous solution at physiological pH (>7 days, fetal bovine serum), and its delivery can be imaged by positron emission tomography (PET). Compound **1** is synthesized in two steps, and employs rapid, late-stage aqueous isotopic exchange ^{18}F-radiochemistry. PET is used to image the in vivo delivery of [^{18}F]-**1** to the murine central nervous system via convection enhanced delivery.

KEYWORDS: *positron emission tomography, drug delivery, glioblastoma, histone deacetylase, panobinostat, imaging*

High grade brain tumors, like diffuse intrinsic pontine glioma (DIPG), have high mortality rates, are inoperable, and do not respond to chemotherapy. DIPG is especially morbid, as it appears during childhood and has a very short median survival of 1 year.[1] There are no known survivors of a DIPG diagnosis. Effective chemotherapeutics for curing DIPG do not currently exist, despite numerous clinical trials.[2] A recent multicenter drug screening study has identified the HDAC inhibitor panobinostat, as a compound with particular promise in the treatment of high grade glioma.[3]

Trials for brain cancer are traditionally performed with oral or intravenous dosing, where systemic drug delivery into the brain can be impaired by the blood−brain barrier (BBB). The high failure rate of drugs in brain tumor trials are often attributed to the impermeability of the BBB.[4−6] Unfortunately, panobinostat bears a limited solubility and a limited ability to cross the BBB.[7] To overcome this issue, several alternative drug delivery strategies are being investigated, such as convection enhanced delivery (CED), transient osmotic disruption of the BBB, inhibition of membrane efflux pumps, intra-arterial, and intranasal chemotherapy.[4−6] These interventions are new and would benefit from technologies that allow us to quantitate and monitor effective drug delivery across physiological barriers.

Positron emission tomography (PET) labeled probes that allow the evaluation of nanomolar drug distribution are an active field of research. The development of PET-labeled HDAC inhibitors include [^{18}F]-fluoroacetamide-1-hexanoicanilide (FAHA), [^{11}C]-MS-275,[8−10] and [^{18}F]-fluoroacetamide-1-hexanoicanilide hydroxamic acid (SAHA).[11] [^{18}F]-panobinostat has not been described.

Received: November 14, 2017
Accepted: January 8, 2018
Published: January 17, 2018

DOI: 10.1021/acsmedchemlett.7b00471
ACS Med. Chem. Lett. 2018, 9, 114−119

Scheme 1. Syntheses of ^{19}F-*N*-Ammoniomethyltrifluoroborate Panobinostat; Ammoniomethyltrifluoroborate ($AMBF_3$), 1; *N*-methyl ammoniomethyltrifluoroborate, 2; and 2-(Bromomethyl)-4,4,5,5-tetraphenyl-1,3,2-dioxaborolane, 4[a,b]

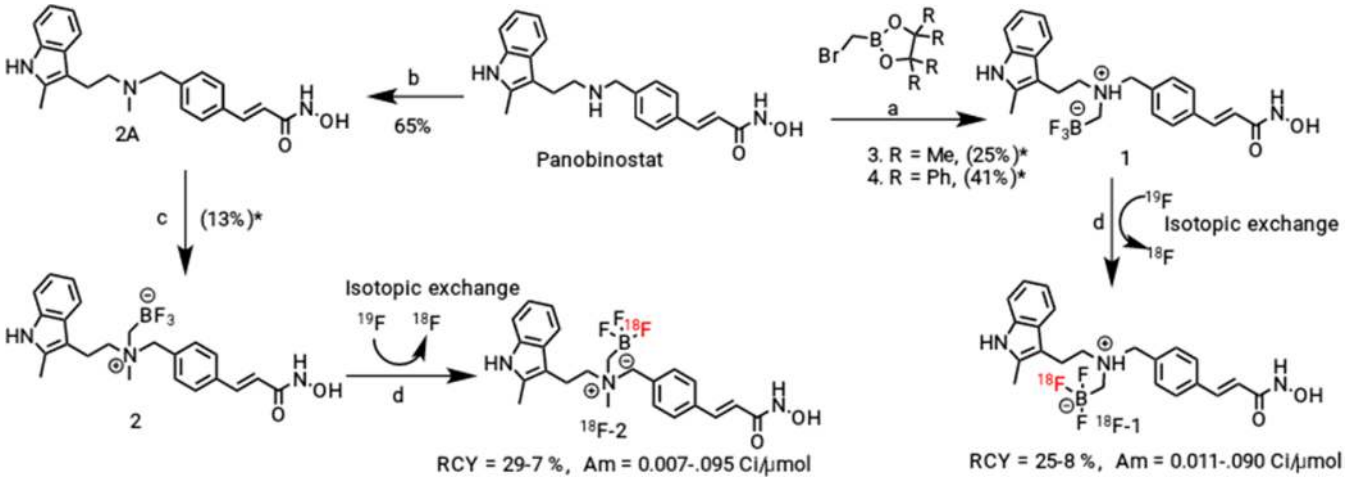

[a]Reagents and conditions: (a) 1.1 equiv of bromomethylboronic acid pinacol ester, 1.1 equiv of DIPEA, DMF/THF (2:1), rt, 4 h, (2) 3 M KHF_2, 1 M HCl, rt, 1 h; (b) HCHO, 2.5 equiv of $Na(OAc)_3BH$; (c) (1) 1.1 equiv of bromomethylboronic acid pinacol ester, DIPEA, DMF/THF (2:1), rt, (2) 3 M KHF_2, 1 M HCl, 0 °C to rt, 1 h; (d) 1 M pyridazine−HCl buffer (pH = 2.5), aq ^{18}F (1.0 mci/μL), 80 °C, 20−30 min. [b]RCY = radiochemical yield, Am = molar activity.

To allow researchers to quantitate advanced methods of delivery to brain tumors, we report the synthesis and radiolabeling of ^{18}F-ammoniomethyltrifluoroborate−panobinostat for PET-guided delivery. This ^{18}F-fluoride bearing derivative of panobinostat differs from previously reported ^{11}C-carbon-labeled panobinostat derivatives.[7,12] The longer half-life of ^{18}F-fluoride ($t_{1/2}$ = 110 min) allows for longer imaging sessions and is accommodative of unforeseen delays that can be common in neurosurgery. Additionally, we incorporate boron-based, aqueous fluoride capture technology onto panobinostat in a radiolabeling strategy that proceeds in one step through water-insensitive, isotopic-exchange (IE).[13−23] Purification is performed through precipitation in a relatively simple strategy for generating ^{18}F-radiolabeled panobinostat.

The reported synthesis of [^{18}F]-**1** describes a PET-active, chemotherapeutic drug that nearly matches the sensitivity, antitumor activities, and mechanisms of unmodified panobinostat (Farydak, Novartis) in DIPG and U87 glioma. This agent is visible by PET, allowing for quantitation of in vivo drug delivery and clearance in novel drug delivery methods, such as CED.[24] New drug delivery strategies are relevant, as CED is recommended for panobinostat.[3]

RESULTS AND DISCUSSION

Oral panobinostat (Farydak) is a HDAC inhibitor that is approved for multiple myeloma in combination with bortezomib and dexamethasone. Panobinostat is a nonselective inhibitor with multiple pathways of antitumor activity.[7,8] Two trifluoroborate-bearing derivatives of panobinostat have been synthesized and studied (Scheme 1). The first panobinostat derivate, **1**, is highly active. Compound **1** bears an *N*-trialkyl-substituted ammoniomethyltrifluoroborate. A second panobinostat derivative, **2**, bears an *N*-tetraalkyl-substituted (quaternary) ammoniomethyltrifluoroborate ($AMBF_3$). Although **1** and **2** are structurally similar, **2** is >20-fold less active than **1** in DIPG cell lines. Compounds **1** and **2** are both generated by alkylating a secondary amine present on panobinostat.

Initial attempts for the synthesis of **1** were performed with bromomethylboronic acid tetramethylpinacol ester, **3**, as an alkylating agent (a synthon previously described by Perrin et al.).[13] Alkylation, followed by a potassium hydrogen fluoride workup (KHF_2 (1 M) in 3 M HCl), gives **1** as a minor product (25%). Yields of **1** could be improved significantly when the bromomethyl boronic acid alkylating agent is substituted for a sterically hindered bromomethyl boronic ester. Reaction of diisopropyl (bromomethyl)boronate with 1,1,2,2-tetraphenyl-1,2-ethanediol at 120 °C in toluene gives 2-(bromomethyl)-4,4,5,5-tetraphenyl-1,3,2-dioxaborolane, **4** (solid, 62% yield) (Supporting Information). Alkylation of panobinostat with **4**, followed by KHF_2 deprotection, gives **1** at improved yield (41%, vs tetramethylpinacol ester[13]). Indole−amine protection is not necessary in the synthesis of **1** when **4** is used as an alkylating agent. Proof of alkylation at the secondary amine (and not the indole) is demonstrated in comprehensive ^{1}H, ^{13}C, HSQC, and HMBC NMR spectroscopy (Supporting Information). Compound **2** was synthesized from an *N*-methylated panobinostat precursor. Panobinostat was alkylated through reductive amination using formaldehyde solution (37%) and sodium triacetoxyborohydride. The isolated product was reacted with bromomethyl boronate and fluoridated with KHF_2 (1 M) and HCl (3 M) in the same pot to give **2** (13%). A quaternary amine is isolated as demonstrated by comprehensive ^{1}H, ^{13}C, HSQC, and HMBC NMR spectroscopy (Supporting Information). Product corresponding to alkylation at the indole−amine is not isolated. Compounds **1** and **2** are stable in physiological solution. Compound instability/fluoride loss/deboronation is not observed when **1** and **2** are incubated in phosphate buffered saline (1x PBS, a phosphate buffer concentrated at 10 mM, containing, 137 mM sodium chloride, pH 7.4 ± 0.2 (25 °C))/fetal bovine serum (FBS) at pH 7.4) for >7 days, in ^{19}F-NMR stability studies[15,25] ($t_{1/2}$ defluoridation >7 days, see the Supporting Information).

Radiochemistry. Aqueous IE based radiolabeling of **1** and **2** proceed best when small total volumes (<50 μL) of ^{18}F-fluoride-ion containing water are employed. Many cyclotrons and commercial suppliers already provide fluoride-ion-contain-

DOI: 10.1021/acsmedchemlett.7b00471
ACS Med. Chem. Lett. 2018, 9, 114−119

ing water at high specific concentration (~1 mCi/μL). These solutions can be used as is, without concentration. Radiosyntheses are initiated (i.e., the time of synthesis (TOS) = 0 min) with the addition of ~10 to 15 μL of concentrated, but not fully evaporated, ^{18}F-fluoride-ion-containing water to solutions of **1** and **2**. Reactions are performed with ~35 mCi of radioactivity in 1500 μL polypropylene tubes. It is recommended that one begin synthesis with at least 90 μg of compound ^{19}F-**1** or ^{19}F-**2**, dissolved in 10 μL of DMSO. Although lesser quantities of ^{19}F-**1** or ^{19}F-**2** would improve radiosynthetic molar activity in IE experiments, these lesser quantities of ^{19}F-**1** or ^{19}F-**2** approach the solubility product constant (K_{sp}) of panobinostat in deionized water. Therefore, purification through precipitation, as described, may not be used to purify lesser quantities of [^{18}F]-**1** or [^{18}F]-**2**. An acid catalyst was required to facilitate fluoride IE. As described in Liu et al.,[13] 10 μL of aqueous pyridazine HCl (1.25 M, pH 2.5) and heating at 80 °C for 25 min facilitate IE. Full solubility of **1** and **2** is observed upon heating.

Isolation of pure [^{18}F]-**1** or [^{18}F]-**2** is achieved by removing unreacted, contaminating ^{18}F-fluoride-ion. Room temperature deionized water (1.3 mL) is added to the labeling mixture, also at room temperature. This results in instantaneous precipitate formation. [^{18}F]-**1** and **2** are pelleted by centrifugation at 18000*g* for 1 min. Supernatant containing contaminating ^{18}F-fluoride ion was decanted and 10 μL of DMSO was added to fully resuspend the [^{18}F]-**1** and **2** containing pellet. This wash process was repeated three more times to completely remove ^{18}F-fluoride ion from [^{18}F]-**1** or **2**. In a typical experiment, 6.2 mCi or 49 mCi/μmol of [^{18}F]-**1** and 5.5 mCi or 45 mCi/μmol of [^{18}F]-**2** are obtained as pure solids. Total synthesis time was 25 min, while purification takes 15 min.

Like panobinostat, [^{18}F]-**1** and **2** are highly insoluble in aqueous solution. [^{18}F]-**1** or **2** must be formulated in 1% DMSO containing 1× PBS for in vivo experiments. This formulation is compatible with direct intracranial injection.[26] To formulate [^{18}F]-**1** or **2**, DMSO (~20 μL) must first be added to the pellet, to fully solubilize [^{18}F]-**1** or **2**. Subsequent addition of PBS (580 μL) will result in a saturated 1% DMSO solution. Precipitates ([^{18}F]-**1** or **2**) will be present and must be removed through centrifugation. Typically, ~300 μCi of a 4 mCi pellet (7.5%, ~ 16 nmols, 27 μM) was solubilized in a 600 μL a 1% DMSO 10 mM/1× PBS solution. Higher percentages of DMSO can be used to solubilize greater activities of [^{18}F]-**1** or **2**, however large percentages of DMSO are not biocompatible, and pure solutions of DMSO are toxic for the central nervous system (CNS). Reversed-phase HPLC analysis was used to confirm [^{18}F]-**1** or **2** radiolabeling and purity (Figure 1).

In Vitro Bioactivity. Panobinostat can be alkylated at its secondary amine without affecting bioactivity.[27] Panobinostat (control), **1**, and **2** are tested for their ability to affect the viability of DIPG-IV, DIPG-XIII, and U87 (glioblastoma) cells. Cell viability assays (CellTiter-Glo, Promega, catalog no. G7572) are performed on U87 and normal astrocytes (control) to demonstrate unmodified panobinostat bioactivity and compound selectivity toward diseased cell lines. At 48 (Figure 2) and 96 h (Supporting Figure S1), **1** demonstrates a bioactivity against DIPG cells that is similar to unmodified panobinostat (Figure 3).[3] Compound **2** demonstrates significantly reduced bioactivity against all cell lines, with micromolar IC_{50} values vs panobinostat's nanomolar values. Panobinostat, **1**, and **2** are selective toward DIPG-IV and DIPG-XIII cells and

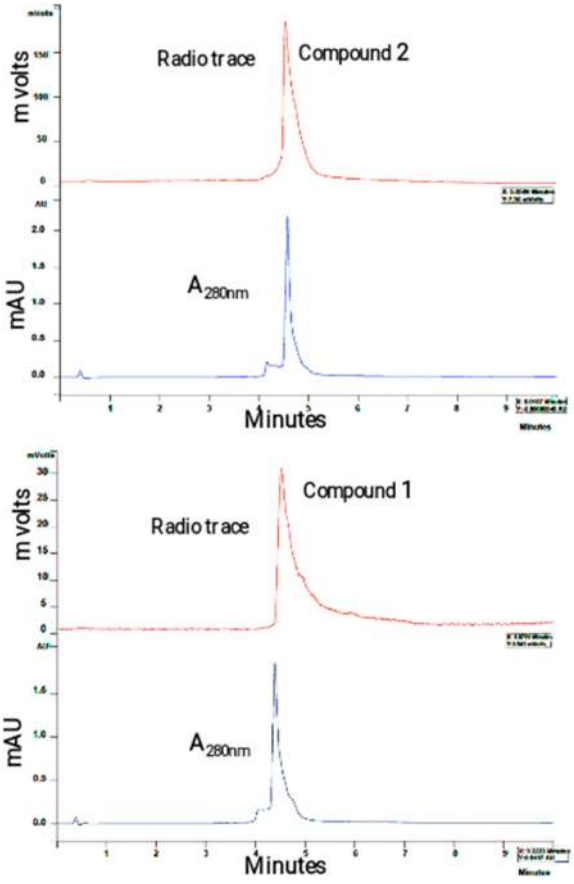

Figure 1. Radio-HPLC confirms the purity of [^{18}F]-**1** and **2**. (B) Reversed-phase HPLC of radiolabeled [^{18}F]-**1** and [^{18}F]-**2** on a Varian HPLC equipped with a Waters SunfireTM C18 3.5 μm 4.6 × 50 mm column (186002551), was used to demonstrate a pure synthesis of [^{18}F]-**1** and **2**. Elution using a 10−90% H_2O/ACN (0.05% TFA), 10 min gradient with a flow rate of 2 mL/min demonstrate a pure synthesis with minimal contaminating fluoride (fluoride would appear between 0 and 1 min).

show a reduced toxicity toward U87 and normal astrocytes. Minimal bioactivity (μM) is exhibited toward normal, non-diseased, control astrocytes across the three compounds; i.e., all three compounds show low toxicity toward astrocytes that line the normal brain parenchyma (Table 1).

The effects of panobinostat, **1**, and **2** on U87 cell proliferation are shown in Figure 3A. Panobinostat and its analogues reduce U87 cell proliferation vs normal cell control. As expected, panobinostat-mediated inhibition of proliferation was more pronounced than that of compounds **1** and **2** at 200 nM. This is consistent with cell viability data described in Figure 2.

To demonstrate that compounds **1** and **2** have an unchanged mechanism of action relative to panobinostat (i.e, panobinostat's mechanism of action is preserved despite chemical modification), DIPG Western blot histone H3 acetylation (acetyl-H3) and cell cycle analyses are performed. In Western blots (Figure 3B), panobinostat treatment induces significant H3 acetylation. This was observed in cells that are treated with **1** and **2** (100 nM, 24 h). To confirm that **1** and **2** have a mechanism of action that is unchanged from panobinostat, cell cycle analyses of panobinostat, **1**, **2**, and untreated U87 cells are conducted (200 nM, 48 h). U87 cell cycle arrest was similar for all 3 compounds at submicromolar concentration. As shown in

DOI: 10.1021/acsmedchemlett.7b00471
ACS Med. Chem. Lett. 2018, 9, 114−119

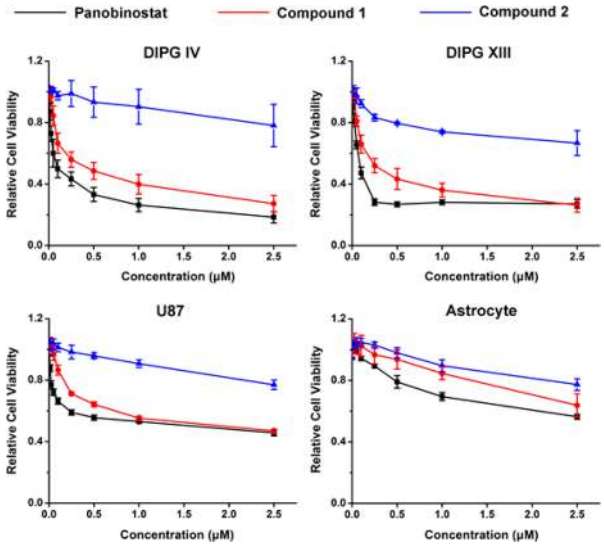

Figure 2. In vitro bioactivity of the unmodified (parent) panobinostat and its two analogues after 48-h exposure. Compound **1** has bioactivity similar to that of unmodified panobinostat against all cell lines (Table 1) and is especially active against pediatric glioma lines DIPG IV and DIPG XIII.

Figure 3C, an enhanced accumulation of sub diploid population was observed in cells either treated with panobinostat, **1** and **2**, suggesting apoptosis. Panobinostat, **1** and **2**, also induce significant G2/M cell cycle arrest, which is consistent with a report by Pettazzoni et al., where G2/M arrest was observed in panobinostat treated prostate cancer cells.[28]

In Vivo Imaging. Neurooncologists and neurosurgeons recommend convection enhanced delivery (CED) for treating DIPG with panobinostat.[3] Compound **1** demonstrates both nanomolar bioactivity against DIPG cells and bears a positron emitting isotope for PET imaging. These properties make compound **1** an ideal candidate for evaluating different methods of HDAC delivery in vivo. Solutions of [^{18}F]-**1** (300 μCi, in 1% DMSO/1× PBS) are delivered to mice through different methods, including CED,[26] to illustrate the use of quantitative imaging in drug delivery, [^{18}F]-**1** was delivered to naive mice by CED,[26] intraperitoneally (Figure 4), and intravenously (IV, not shown).

As expected, CED was the superior method for delivering large doses of [^{18}F]-**1** to the brain. In Figure 4, compound [^{18}F]-**1** was delivered at high concentration to the brain, via CED, and is retained in the brain for at least 1 h. In comparative studies where [^{18}F]-**1** was delivered intraperitoneally or intravenously, very little [^{18}F]-**1** was detected in the brain post injection,[12] even after [^{18}F]-**1** was allowed to distribute for 4 h. PET imaging also allows for dynamic monitoring of delivery and clearance. As shown in Supporting Figure S2, 2 mm diameter, elliptical, regions-of-interest (4.19 μL, ROI) are placed over the site of injection to image drug delivery. CED was 120 times more effective at delivering [^{18}F]-**1** panobinostat to the pons in naïve mice. [^{18}F]-**1** panobinostat clears from the brain quickly. At 240 min post injection, the concentration of [^{18}F]-**1** remains 44.6-fold higher in the pons vs intraperitoneal injection.

DISCUSSION

In this study, we demonstrate simplified radiochemistry for transforming the HDAC inhibitor panobinostat into an agent

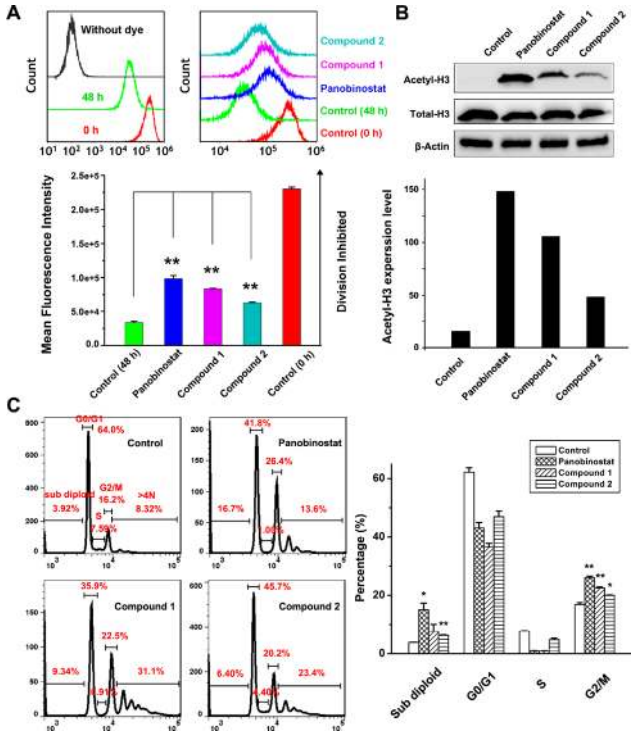

Figure 3. Assays that compare biological activity between panobinostat and its analogues (**1** and **2**) on U87 and DIPG biological activity. (A) Panobinostat and analogue impact on U87 cell proliferation. Cells are stained with a proliferation tracking dye (CellTraceTM Far Red) prior to treatment with 200 nM drug for 48 h. (B) Western blot analysis showing panobinostat and analogue impact on DIPG IV acetyl-H3 expression in cells. DIPG IV cells are treated with 100 nM panobinostat, **1**, and **2** for 24 h and are analyzed for changes in acetyl-H3 expression. The total histone H3 (Total-H3) and β-actin content serve as controls. (C) Panobinostat and analogues impact on U87 cell-cycle. Cell cycle status was determined by staining treated cells (200 nM) with propidium iodine before fluorescence activated sorting analysis (FACS). The percentage of cells in sub diploid (apoptosis), G0/G1, S, and G2/M phases are shown in representative histograms (left) and are summarized as mean ± SD in right. *Represents a statistically significant difference between control group and treatment group (*: $p < 0.05$, **: $p < 0.01$).

Table 1. Inhibitory Profile of Panobinostat Derivatives 1 and 2 and against Glioma Cell Lines IC_{50} (nM) after 48 h Exposure

compd	DIPG-IV	DIPG-XIII	U87	astrocytes
panobinostat	64	38	65	76
1	122	108	212	5265
2	4358	310	4483	5125

[a]Mean from three different cell viability assays (standard error is in the range of ±2−5% of reported IC_{50}).

that can be imaged by ^{18}F-PET. This labeled HDAC inhibitor could be used by itself or in combination with panobinostat to treat and explore new routes of drug delivery in the treatment of cancer. We look forward to using compounds **1** and **2** in identifying new routes of drug delivery, combining old routes of delivery, and in quantitatively comparing advanced strategies to standard (intravenous, peritoneal, and intradermal) modes of drug delivery. The synthesis of **1** was performed in 2 steps from commercially available panobinostat. The ^{18}F-radiolabeling and generation of millicurie amounts of [^{18}F]-**1** is performed under

DOI: 10.1021/acsmedchemlett.7b00471
ACS Med. Chem. Lett. 2018, 9, 114−119

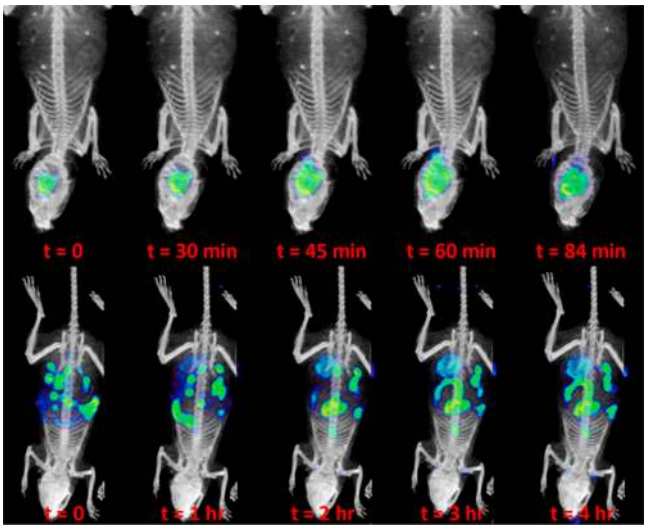

Figure 4. Panobinostat compound [^{18}F]-**1** allows for real time, *in vivo* imaging of drug delivery via CED (top) or IP delivery (bottom). The former achieves delivery of greater concentrations of panobinostat to the brain. [^{18}F]-**1** PET allows quantitation of drug delivery and clearance (see the Supporting Information) of both delivery mechanisms.

acidic, IE conditions where a nonradioactive ^{19}F atom on compound **1** and **2** was exchanged with ^{18}F-fluoride ion in acidic water. Compounds **1** and **2** are stable at physiological pH. In our hands, [^{18}F]-**1** radiolabeling was infallible (a 100% success rate was observed) when reactions are performed with aqueous specific concentrations of ~1 mCi/μL. In employing trifluoroborate IE technology, the nonradioactive starting compound ^{19}F-**1** is electronically identical to its radioactive ^{18}F counterpart, therefore advanced chromatographic separation is not needed to remove precursor, and simple precipitation could be used to isolate pure samples of [^{18}F]-**1**. Radiochemical yields and molar activities range from 96 ± 10 mCi/μmol (decay uncorrected). The radiochemical precursor ^{19}F-**1** is useful in pharmacological assays (Figure 3) as is, without manipulation.

Radiochemical approaches are needed to study the accumulation of effective nanomolar anticancer drugs at the site of disease. These approaches would allow immediate determination of accurate drug delivery and clearance, providing crucial data in redosing. Using [^{18}F]-**1**, cases of missed HDAC delivery can be immediately recognized by PET/CT or PET/MR, allowing for prompt intervention in the case of failed or inaccurate delivery. Currently, real-time imaging is not used to confirm drug delivery. Without drugs like [^{18}F]-**1**, inaccurate drug delivery cannot be immediately recognized. One would currently realize drug misdelivery by observing significant disease progression, after the window for meaningful intervention has passed.[29] By imaging delivery with agents like [^{18}F]-**1**, symptoms of inaccurate drug delivery will no longer be incorrectly interpreted as a lack of drug efficacy.

CONCLUSIONS

Here, we report the synthesis and radiolabeling of a nanomolar analog of panobinostat that bears ^{18}F-fluoride, allowing the delivery of [^{18}F]-**1** to be imaged by PET. Like the parent drug, panobinostat, **1** is found to inhibit the growth of DIPG IV, XIII, and U87 cells at nanomolar concentration, while leaving normal astrocytes unaffected. A close structural analog **2**, does not demonstrate the same inhibitory activity. Compound **1** is relevant because of its newfound importance in glioma.[3] The use of [^{18}F]-**1** in PET allows for noninvasive, quantitative, image-guided HDAC inhibitor delivery at high resolution.[30] PET imaging would promptly identify cases of missed or inadequate HDAC inhibitor delivery in a patient.

ASSOCIATED CONTENT

Supporting Information

The Supporting Information is available free of charge on the ACS Publications website at DOI: 10.1021/acsmedchemlett.7b00471.

Methods for panobonostat−AMBF$_3$ preparation, characterization, in vitro stability verification, and in vivo data (PDF)

AUTHOR INFORMATION

Corresponding Author

*E-mail: rct2001@med.cornell.edu. Phone: (+1) (646) 962-6195.

ORCID

Umberto Tosi: 0000-0003-0847-2400

Richard Ting: 0000-0003-2096-5232

Author Contributions

The manuscript was written through contributions of all authors. All authors have given approval to the final version of the manuscript.

Funding

The project was supported by grants by the National Institute of Biomedical Imaging and Bioengineering K99/R00 (EB013904), the Alex Lemonade Stand Foundation for Childhood Cancer, the Matthew Larson Foundation for Pediatric Brain Tumors Research Grant, The Cristian Rivera Foundation grant, a St. Baldrick's Summer Fellow Grant, and a US Department of Defense Congressionally Directed Research Projects Special Emphasis Grant on Pediatric Brain Tumors (CA160373).

Notes

The authors declare no competing financial interest.

ACKNOWLEDGMENTS

We thank Dr. Michelle Monje of Stanford University for providing SU-DIPG-IV and SU-DIPG-XIII cells.

ABBREVIATIONS

AMBF$_3$, alkylammoniomethyltrifluoroborate; CED, convention enhanced delivery; HDAC, histone deacetylase; PET, positron emission tomography; CT, computed tomography; DIPEA, *N*,*N*-diisopropylethylamine; EDCI, 1-ethyl-3-(3-(dimethylamino)propyl)carbodiimide

REFERENCES

(1) Ostrom, Q. T.; de Blank, P. M.; Kruchko, C.; Petersen, C. M.; Liao, P.; Finlay, J. L.; Stearns, D. S.; Wolff, J. E.; Wolinsky, Y.; Letterio, J. J.; Barnholtz-Sloan, J. S. Alex's Lemonade Stand Foundation Infant and Childhood Primary Brain and Central Nervous System Tumors Diagnosed in the United States in 2007−2011. *Neuro-Oncology* **2015**, *16* (suppl_10), x1−x36.

(2) Jones, C.; Karajannis, M. A.; Jones, D. T. W.; Kieran, M. W.; Monje, M.; Baker, S. J.; Becher, O. J.; Cho, Y. J.; Gupta, N.; Hawkins, C.; Hargrave, D.; Haas-Kogan, D. A.; Jabado, N.; Li, X. N.; Mueller, S.;

DOI: 10.1021/acsmedchemlett.7b00471
ACS Med. Chem. Lett. 2018, 9, 114−119

Nicolaides, T.; Packer, R. J.; Persson, A. I.; Phillips, J. J.; Simonds, E. F.; Stafford, J. M.; Tang, Y.; Pfister, S. M.; Weiss, W. A. Pediatric high-grade glioma: biologically and clinically in need of new thinking. *Neuro Oncol.* **2017**, *19* (2), 153−161.
(3) Grasso, C. S.; Tang, Y.; Truffaux, N.; Berlow, N. E.; Liu, L.; Debily, M.-A.; Quist, M. J.; Davis, L. E.; Huang, E. C.; Woo, P. J. Functionally defined therapeutic targets in diffuse intrinsic pontine glioma. *Nat. Med.* **2015**, *21* (6), 555−559.
(4) Siegal, T. Which drug or drug delivery system can change clinical practice for brain tumor therapy? *Neuro Oncol* **2013**, *15* (6), 656−69.
(5) Tosi, U.; Marnell, C. S.; Chang, R.; Cho, W. C.; Ting, R.; Maachani, U. B.; Souweidane, M. M. Advances in Molecular Imaging of Locally Delivered Targeted Therapeutics for Central Nervous System Tumors. *Int. J. Mol. Sci.* **2017**, *18* (2), 351.
(6) Goodwin, C. R.; Xu, R.; Iyer, R.; Sankey, E. W.; Liu, A.; Abu-Bonsrah, N.; Sarabia-Estrada, R.; Frazier, J. L.; Sciubba, D. M.; Jallo, G. I. Local delivery methods of therapeutic agents in the treatment of diffuse intrinsic brainstem gliomas. *Clin Neurol Neurosurg* **2016**, *142*, 120−7.
(7) Singleton, W. G.; Collins, A. M.; Bienemann, A. S.; Killick-Cole, C. L.; Haynes, H. R.; Asby, D. J.; Butts, C. P.; Wyatt, M. J.; Barua, N. U.; Gill, S. S. Convection enhanced delivery of panobinostat (LBH589)-loaded pluronic nano-micelles prolongs survival in the F98 rat glioma model. *Int. J. Nanomed.* **2017**, *12*, 1385−1399.
(8) Hooker, J. M.; Kim, S. W.; Alexoff, D.; Xu, Y.; Shea, C.; Reid, A.; Volkow, N.; Fowler, J. S. Histone deacetylase inhibitor, MS-275, exhibits poor brain penetration: PK studies of [C]MS-275 using Positron Emission Tomography. *ACS Chem. Neurosci.* **2010**, *1* (1), 65−73.
(9) Reid, A. E.; Hooker, J.; Shumay, E.; Logan, J.; Shea, C.; Kim, S. W.; Collins, S.; Xu, Y.; Volkow, N.; Fowler, J. S. Evaluation of 6-([(18)F]fluoroacetamido)-1-hexanoicanilide for PET imaging of histone deacetylase in the baboon brain. *Nucl. Med. Biol.* **2009**, *36* (3), 247−58.
(10) Yeh, H. H.; Tian, M.; Hinz, R.; Young, D.; Shavrin, A.; Mukhapadhyay, U.; Flores, L. G.; Balatoni, J.; Soghomonyan, S.; Jeong, H. J.; Pal, A.; Uthamanthil, R.; Jackson, J. N.; Nishii, R.; Mizuma, H.; Onoe, H.; Kagawa, S.; Higashi, T.; Fukumitsu, N.; Alauddin, M.; Tong, W.; Herholz, K.; Gelovani, J. G. Imaging epigenetic regulation by histone deacetylases in the brain using PET/MRI with (1)(8)F-FAHA. *NeuroImage* **2013**, *64*, 630−9.
(11) Hendricks, J. A.; Keliher, E. J.; Marinelli, B.; Reiner, T.; Weissleder, R.; Mazitschek, R. In vivo PET imaging of histone deacetylases by 18F-suberoylanilide hydroxamic acid (18F-SAHA). *J. Med. Chem.* **2011**, *54* (15), 5576−82.
(12) Wang, C.; Eessalu, T. E.; Barth, V. N.; Mitch, C. H.; Wagner, F. F.; Hong, Y.; Neelamegam, R.; Schroeder, F. A.; Holson, E. B.; Haggarty, S. J.; Hooker, J. M. Design, synthesis, and evaluation of hydroxamic acid-based molecular probes for in vivo imaging of histone deacetylase (HDAC) in brain. *Am. J. Nucl. Med. Mol. Imaging* **2013**, *4* (1), 29−38.
(13) Liu, Z. B.; Pourghiasian, M.; Radtke, M. A.; Lau, J.; Pan, J. H.; Dias, G. M.; Yapp, D.; Lin, K. S.; Benard, F.; Perrin, D. M. An Organotrifluoroborate for Broadly Applicable One-Step F-18-Labeling. *Angew. Chem., Int. Ed.* **2014**, *53* (44), 11876−11880.
(14) Liu, Z.; Lin, K. S.; Benard, F.; Pourghiasian, M.; Kiesewetter, D. O.; Perrin, D. M.; Chen, X. One-step (18)F labeling of biomolecules using organotrifluoroborates. *Nat. Protoc.* **2015**, *10* (9), 1423−32.
(15) Liu, Z.; Chao, D.; Li, Y.; Ting, R.; Oh, J.; Perrin, D. M. From minutes to years: predicting organotrifluoroborate solvolysis rates. *Chem. - Eur. J.* **2015**, *21* (10), 3924−8.
(16) Ting, R.; Harwig, C.; auf dem Keller, U.; McCormick, S.; Austin, P.; Overall, C. M.; Adam, M. J.; Ruth, T. J.; Perrin, D. M. Toward [18F]-labeled aryltrifluoroborate radiotracers: in vivo positron emission tomography imaging of stable aryltrifluoroborate clearance in mice. *J. Am. Chem. Soc.* **2008**, *130* (36), 12045−55.
(17) Liu, Z.; Chen, H.; Chen, K.; Shao, Y.; Kiesewetter, D. O.; Niu, G.; Chen, X. Boramino acid as a marker for amino acid transporters. *Sci. Adv.* **2015**, *1* (8), e1500694.
(18) Kommidi, H.; Guo, H.; Chen, N.; Kim, D.; He, B.; Wu, A. P.; Aras, O.; Ting, R. An [18F]-Positron-Emitting, Fluorescent, Cerebrospinal Fluid Probe for Imaging Damage to the Brain and Spine. *Theranostics* **2017**, *7* (9), 2377−2391.
(19) Schirrmacher, R.; Bradtmoller, G.; Schirrmacher, E.; Thews, O.; Tillmanns, J.; Siessmeier, T.; Buchholz, H. G.; Bartenstein, P.; Wangler, B.; Niemeyer, C. M.; Jurkschat, K. 18F-labeling of peptides by means of an organosilicon-based fluoride acceptor. *Angew. Chem., Int. Ed.* **2006**, *45* (36), 6047−50.
(20) Bernard-Gauthier, V.; Bailey, J. J.; Liu, Z.; Wangler, B.; Wangler, C.; Jurkschat, K.; Perrin, D. M.; Schirrmacher, R. From Unorthodox to Established: The Current Status of (18)F-Trifluoroborate- and (18)F-SiFA-Based Radiopharmaceuticals in PET Nuclear Imaging. *Bioconjugate Chem.* **2016**, *27* (2), 267−79.
(21) Lindner, S.; Michler, C.; Leidner, S.; Rensch, C.; Wangler, C.; Schirrmacher, R.; Bartenstein, P.; Wangler, B. Synthesis and in vitro and in vivo evaluation of SiFA-tagged bombesin and RGD peptides as tumor imaging probes for positron emission tomography. *Bioconjugate Chem.* **2014**, *25* (4), 738−49.
(22) Bernard-Gauthier, V.; Wangler, C.; Schirrmacher, E.; Kostikov, A.; Jurkschat, K.; Wangler, B.; Schirrmacher, R. (1)(8)F-labeled silicon-based fluoride acceptors: potential opportunities for novel positron emitting radiopharmaceuticals. *BioMed Res. Int.* **2014**, *2014*, 454503.
(23) Wangler, C.; Niedermoser, S.; Chin, J.; Orchowski, K.; Schirrmacher, E.; Jurkschat, K.; Iovkova-Berends, L.; Kostikov, A. P.; Schirrmacher, R.; Wangler, B. One-step (18)F-labeling of peptides for positron emission tomography imaging using the SiFA methodology. *Nat. Protoc.* **2012**, *7* (11), 1946−55.
(24) Souweidane, M. M. Editorial: Convection-enhanced delivery for diffuse intrinsic pontine glioma. *J. Neurosurg Pediatr* **2014**, *13* (3), 273−4.
(25) Ting, R.; Harwig, C. W.; Lo, J.; Li, Y.; Adam, M. J.; Ruth, T. J.; Perrin, D. M. Substituent effects on aryltrifluoroborate solvolysis in water: implications for Suzuki-Miyaura coupling and the design of stable (18)F-labeled aryltrifluoroborates for use in PET imaging. *J. Org. Chem.* **2008**, *73* (12), 4662−70.
(26) Wang, M.; Kommidi, H.; Tosi, U.; Guo, H.; Zhou, Z.; Schweitzer, M. E.; Wu, L. Y.; Singh, R.; Hou, S.; Law, B.; Ting, R.; Souweidane, M. M., A murine model for quantitative, real-time evaluation of convection-enhanced delivery (RT-CED) using an ^{18}[F]-positron emitting, fluorescent derivative of dasatinib. *Mol. Cancer Ther.* **2017**.16290210.1158/1535-7163.MCT-17-0423
(27) Meng, Q.; Liu, Z.; Li, F.; Ma, J.; Wang, H.; Huan, Y.; Li, Z. An HDAC-Targeted Imaging Probe LBH589-Cy5.5 for Tumor Detection and Therapy Evaluation. *Mol. Pharmaceutics* **2015**, *12* (7), 2469−76.
(28) Pettazzoni, P.; Pizzimenti, S.; Toaldo, C.; Sotomayor, P.; Tagliavacca, L.; Liu, S.; Wang, D.; Minelli, R.; Ellis, L.; Atadja, P.; Ciamporcero, E.; Dianzani, M. U.; Barrera, G.; Pili, R. Induction of cell cycle arrest and DNA damage by the HDAC inhibitor panobinostat (LBH589) and the lipid peroxidation end product 4-hydroxynonenal in prostate cancer cells. *Free Radical Biol. Med.* **2011**, *50* (2), 313−22.
(29) Cawthorne, C.; Burrows, N.; Gieling, R. G.; Morrow, C. J.; Forster, D.; Gregory, J.; Radigois, M.; Smigova, A.; Babur, M.; Simpson, K.; Hodgkinson, C.; Brown, G.; McMahon, A.; Dive, C.; Hiscock, D.; Wilson, I.; Williams, K. J. [18F]-FLT positron emission tomography can be used to image the response of sensitive tumors to PI3-kinase inhibition with the novel agent GDC-0941. *Mol. Cancer Ther.* **2013**, *12* (5), 819−28.
(30) An, F. F.; Chan, M.; Kommidi, H.; Ting, R. Dual PET and Near-Infrared Fluorescence Imaging Probes as Tools for Imaging in Oncology. *AJR, Am. J. Roentgenol.* **2016**, *207* (2), 266−273.

DOI: 10.1021/acsmedchemlett.7b00471
ACS Med. Chem. Lett. 2018, 9, 114−119